Stability of Time-Invariant Extremum Seeking Control for Limit Cycle Minimization

Saurav Kumar[1], Oleg Makarenkov[2], Robert D. Gregg[3], and Nicholas Gans[4]

***Abstract*—This paper presents a time-invariant extremum seeking controller (ESC) for nonlinear autonomous systems with limit cycles. For this time-invariant ESC, we propose a method to prove the closed loop system has an asymptotically stable limit cycle. The method is based on a perturbation theorem for maps, and, unlike existing techniques that use averaging and singular perturbation tools, it is not limited to weakly nonlinear systems. We use a typical example system to show that our method does indeed establish asymptotic stability of the limit cycle with minimal amplitude. Utilizing the example, we provide a general guide for analytic computations that are required to apply our method. The corresponding Mathematica code is available as supplementary material.**

***Index Terms*—Extremum Seeking Control, Adaptive Control, Autonomous Systems, Limit Cycles, Perturbation Theory**

I. Introduction

Limit cycles occur in numerous engineering applications, e.g., tracking error response in rehabilitation robots [1], self-excited vibrations in automotive braking systems [2], oscillatory wing response in aircraft [3], which can limit the performance and safety of the system. Feedback control can reduce the size of the limit cycle but cannot completely eliminate it. To improve performance, the control requirement is often to enforce a "smallest", stable limit cycle.

Model-free approaches such as extremum seeking control (ESC) can be deployed to optimize the performance of the system. A conventional perturbation-based ESC [4], [5] was used to minimize the size of the limit cycles of such systems in real-time [1], [6]–[9]. Conventional perturbation-based ESC schemes use a slow, exogenous *time-dependent* periodic signal such as $d(t) = a \sin \omega t$, known as the dither signal, to estimate the local gradient and optimize the steady-state objective of a plant with unknown dynamics [1], [4], [5], [10]. From hereon, we refer to such schemes as *time-based* ESC. The stability analysis of time-based ESC requires sufficient time-scale separation between the plant and the ESC dynamics and assumes that the plant operates at a fixed time-scale. Accordingly, the dither frequency, ω, is judiciously chosen such that the ESC dynamics are at least an order of magnitude slower than the plant dynamics. In particular, for periodic systems, the dither frequency is chosen to be smaller than the oscillation frequency of the plant states [6].

[1]Robotics Institute, Carnegie Mellon University, Pittsburgh, PA 15213, USA. [2]Department of Mathematical Sciences, The University of Texas at Dallas, Richardson, TX 75080, USA. [3]Department of Electrical and Computer Engineering, The University of Michigan - Ann Arbor, MI 48109, USA. [4]The University of Texas at Arlington Research Institute, University of Texas at Arlington, Arlington, TX 76019, USA. {saravk,rgregg}@ieee.org, makarenkov@utdallas.edu, ngans@uta.edu

This material is based upon work supported by the National Science Foundation (NSF) under Grant No. 1728057 and 1916876.

However, there are applications where the plant does not operate at a fixed time-scale. Human locomotion is one example, which exhibits varying time-scales based on the walking speed) [11]. In a transfemoral powered prosthetic leg, the evolution of the knee and the ankle joints are typically synchronized to an external signal, e.g., the human's hip signal [12], [13]. In the application of *time-based* ESC with such periodic systems with varying time-scales, if the desired task results in slow operation speed, then the use of fixed *time-based* ESC parameters would violate the time-scale separation thus, the ESC adaptation can no longer be guaranteed to be stable [14]. Although newer forms of ESC using high-frequency dither signals can handle varying time-scales [15]–[17], the introduction of fast oscillations in the system might be undesirable for precise trajectory tracking applications.

To address the above problem, we proposed in [18] to replace the external *time-dependent* dither signal in conventional ESC structure with a function of the periodic states of the system. We call this ESC scheme, using a state-based dither, *time-invariant* ESC. A mathematically rigorous stability proof of such an ESC scheme has not appeared in the literature yet.

The majority of the theoretical work on proving the stability of *time-based* ESC [4], [6], [10], [19] use averaging and singular perturbation theory to prove the stability, where the dither frequency ω was used as a small singular perturbation parameter. In *time-invariant* ESC, due to the use of *state-based* dither signal, we lose access to the dither frequency ω, and thus, the use of averaging and singular perturbation tools is not trivial. Recently, we demonstrated the stability of limit cycles when using *time-invariant* ESC for weakly nonlinear Van der Pol oscillators [18]. By exploiting the structure of the Van der Pol oscillator, we performed a change of coordinates that transformed the overall system to a form suitable to perform averaging and singular perturbation. However, the limitation of that approach was that stability could only be established for weakly nonlinear oscillators. The proof presented in [18] is heuristic in the sense that the higher order terms of the expansion of the solution of the Van der Pol oscillator, corresponding to the nonlinearity, were truncated.

In this paper, we propose a method to prove asymptotic stability of a time-invariant ESC for nonlinear autonomous systems with limit cycles. Unlike existing techniques utilizing averaging and singular perturbation tools that handle small nonlinearities in the system, our method based on perturbation theorem for maps does not impose this restriction. As an example to illustrate the strength of this method, we choose a so-called *normal form* of a nonlinear system with a limit cycle, which is commonly used when an explicit formula for the limit cycle is required. The method is based on the perturbation theorem for discrete dynamical systems [20], which allows us to investigate bifurcation of asymptotically stable fixed points from a 1-parameter family of fixed points. As the results of [20] are rather abstract, we prove an applicable corollary of the theory of [20], which generalizes the corresponding perturbation result of [21] to arbitrary dimension. The main requirement of our theorem is the knowledge of the parameter-dependent limit cycle of the plant, which is a standard requirement for analytic proofs regarding control of nonlinear systems with a limit cycle; see related results on classical Pyragas control [22]–[24] or transverse linearization [25].

The rest of the paper is organized as follows. In Section II, we present the structure of time-invariant ESC and our problem statement. In Section III, we prove a concise perturbation theorem on bifurcation of fixed points from families of fixed points for general n-dimensional systems. Next, in Section IV, we apply this theorem on a normal form of a nonlinear autonomous system with a limit cycle to prove asymptotic stability of the limit cycle for the closed-loop system. The simulation results are presented next in Section V. Finally, Section VI concludes the paper with discussions.

II. Time-Invariant ESC —Problem Statement

Consider a single-input single output dynamical system

$$\begin{aligned} \dot{x} &= f(x, \theta, v), \\ y_o &= h(x), \end{aligned} \tag{1}$$

where the state $x \in \mathbb{R}^n$, tunable parameter $\theta \in \mathbb{R}$, input $v \in \mathbb{R}$, output $y_o \in \mathbb{R}$, $f : \mathbb{R}^n \times \mathbb{R} \to \mathbb{R}^n$, and $h : \mathbb{R}^n \to \mathbb{R}$. Assume that we know a smooth control law, $v = \alpha(x, \theta)$, such that the closed-loop system

$$\dot{x} = f(x, \theta, \alpha(x, \theta)) \tag{2}$$

has a stable limit cycle for all $\theta \in \mathbb{R}$. The objective of ESC is to tune the controller parameter θ to minimize the "amplitude" of the limit cycle, without the knowledge of the system dynamics (1).

Fig. 1 shows the block diagram of time-invariant ESC, which, as suggested in [18], uses a state-dependent dither signal in contrast to a time-dependent dither $d(t) = a\sin(\omega t)$ in time-based ESC. In order to reduce the amplitude of the state-based dither, $d(x, \theta)$, the approach in [18] suggests to multiply it with a constant $M \in \mathbb{R}_+$, which is added to the current best estimate of θ. The closed-loop system (2) can then be rewritten as

$$\begin{aligned} \dot{x} &= f(x, \theta, \alpha(x, \theta + Md(x, \theta))) \\ y_o &= h(x), \end{aligned} \tag{3}$$

which will generically have stable limit cycles, close to those of (2), for an interval of the values of θ provided that $M \geq 0$ is small, see [26, Ch. 14, Theorems 2.1 and 2.2].

For limit cycle minimization, an amplitude detector was incorporated in the feedback scheme of conventional ESC [6]. The detector consists of a high-pass filter (HPF), squaring function, low-pass filter (LPF), and a gain block, all connected

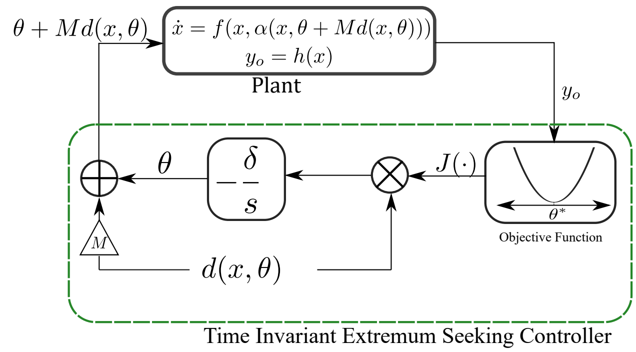

Fig. 1: Block diagram of a *time-invariant* ESC using a state-dependent dither signal $d(x, \theta)$. In order to minimize the size of the limit cycle, we use x_1^2 as the objective function as in [6], [18].

in cascade. Assume that the output y_o of the system in a limit cycle is sinusoidal, $y_o(t) = y_0 + r\sin(\omega t + \phi)$, where y_0, r, ω are constants. The DC component, y_0, is eliminated by the HPF. The output of the HPF is then squared to get $(r^2/2)(1 - \cos 2\omega t)$, which is then passed through the LPF to give $r^2/2$. To extract the amplitude of the limit cycle r, the output of the LPF is then doubled and its square root is taken. This approach can also be used to estimate the amplitude of non-sinusoidal limit cycles. The output measurements is fed to the limit cycle detector block to compute the objective function $J(x)$. The objective function is then multiplied with the same *state-dependent* dither signal $d(x, \theta)$ to get an estimate of its gradient with respect to θ, $\partial J/\partial\theta$. The resulting signal is then integrated and multiplied with gain $-\delta$ to tune θ in the direction of the estimate of $\partial J/\partial\theta$. The dynamics of *time-invariant* ESC are then given by

$$\dot{\theta} = -\delta J(x) d(x, \theta). \tag{4}$$

In Section III, we prove a general theorem (Theorem 1) that for all $\delta > 0$ sufficiently small, the solutions of system (3)-(4) converge asymptotically to a cycle that is δ-close to a so-called *generating cycle* of (3) (see Remark 1 for the definition). The value of θ that corresponds to the generating cycle is denoted in Theorem 1 by θ_0. In Section IV, we use a normal form example (from [27, §2.4]) to prove that such a generating limit cycle is indeed a limit cycle of minimal amplitude in the 2D case. In other words, the normal form example allows us to compute the optimal value of θ directly (which we denote by θ^*), and we then prove that conditions of Theorem 1 hold specifically for $\theta_0 = \theta^*$.

III. The General Result

In order to study limit cycles of system (3)-(4), we consider an n-dimensional Poincaré map $u \mapsto \mathcal{P}(u, \delta)$ of (3)-(4) induced by a cross-section $S = \{x \in \mathbb{R}^{n+1} : x_1 = c\}$, where c is a constant (see [27, §1.5.2]). In particular, the variable u in our analysis is given by $u = (x_2, ..., x_n, \theta)^T$. Stable fixed points of the Poincaré map correspond to the initial conditions of stable limit cycles of (3)-(4). Since system (3) admits a limit cycle x_θ for each θ, the full system (3)-(4) admits a C^1-smooth family of cycles (x_θ, θ) parameterized by θ when δ is set to 0. Therefore, the map $u \mapsto \mathcal{P}(u, 0)$ admits a family of fixed points $(\xi(\theta), \theta)^T$, where $\theta \mapsto \xi(\theta)$ is C^1-smooth. The

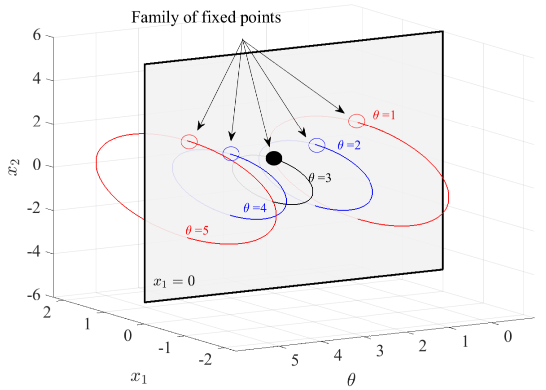

Fig. 2: The family of fixed points for the Poincaré map $(x_2, \theta) \mapsto \mathcal{P}(x_2, \theta, \delta)$ of (10)-(12) at $\delta = 0$ with different initial conditions. The black solid dot represents the fixed point (x_2^*, θ^*). The black cycle corresponding to $\theta = \theta^* = 3$ is the limit cycle of (10)-(11) with minimum amplitude, and the blue and red cycles correspond to $\theta = 2, 4$, and $\theta = 1, 5$, respectively. All other parameters of the system (10)-(12) are same as mentioned in Section V.

analysis in this section will determine when a particular fixed point $(\xi(\theta_0), \theta_0)$ of this family persists and gains asymptotic stability (or disappears) upon varying δ from $\delta = 0$ to $\delta > 0$.

Differentiating

$$\mathcal{P}((\xi(\theta), \theta)^T, 0) = (\xi(\theta), \theta)^T \tag{5}$$

with respect to θ we observe that $\mathcal{P}_u((\xi(\theta), \theta)^T, 0)$ always admits an eigenvalue $\rho_1 = 1$. In what follows, we will write $\mathcal{P}(\xi(\theta), \theta, \delta)$ to denote $\mathcal{P}((\xi(\theta), \theta)^T, \delta)$ to shorten the text. Also, $\mathcal{P}_u$ denotes the derivative of $\mathcal{P}$ with respect to u. Let us fix some $\theta_0 \in \mathbb{R}$ and denote by $\sigma(\mathcal{P}_u(\xi(\theta_0), \theta_0, 0))$ the set of eigenvalues of $\mathcal{P}_u(\xi(\theta_0), \theta_0, 0)$ counting the algebraic multiplicity. Assume that

$$\sigma(\mathcal{P}_u(\xi(\theta_0), \theta_0, 0)) = (1, \rho_2, ..., \rho_n), \quad |\rho_i| \neq 1, \quad i \in \overline{2, n}. \tag{6}$$

Let $y \in \mathbb{R}^n$ denote the eigenvector of $\mathcal{P}_u(\xi(\theta_0), \theta_0, 0)$ that corresponds to the eigenvalue $\rho_1 = 1$. Let $\tilde{y}$ be the $n \times (n-1)$ matrix of $n-1$ eigenvectors of $\mathcal{P}_u(\xi(\theta_0), \theta_0, 0)$ corresponding to the eigenvalues $\rho_2, ..., \rho_n$. Analogously, let $z \in \mathbb{R}^n$ be the eigenvector of $\mathcal{P}_u(\xi(\theta_0), \theta_0, 0)^T$ that corresponds to the eigenvalue 1 and let $\tilde{z}$ be the $n \times (n-1)$ matrix of eigenvectors of $\mathcal{P}_u(\xi(\theta_0), \theta_0, 0)^T$ that corresponds to the eigenvalues not equal to 1.

Theorem 1. *Assume that the following conditions hold for the unperturbed system, i.e., $\delta = 0$ in (3)-(4) in addition to (6):*

$$|\rho_2| < 1, \; ..., \; |\rho_n| < 1, \tag{7}$$

$$z^T \mathcal{P}_\delta(\xi(\theta_0), \theta_0, 0) = 0, \tag{8}$$

$$z^T \mathcal{P}_{\delta u}(\xi(\theta_0), \theta_0, 0) y < 0. \tag{9}$$

Then, for all $\delta > 0$ sufficiently small, the dynamics of the full system (3)-(4) admit an asymptotically stable limit cycle $(x_\delta(t), \theta_\delta(t))$ such that $(x_\delta(0), \theta_\delta(0)) \to (\xi(\theta_0), \theta_0)$ as $\delta \to 0$.

Proof. The proof is given in the appendix. □

Remark 1. *By analogy with [28], the limit cycle of (3) corresponding to some $\theta = \theta_0$ is termed a "generating limit cycle" if it satisfies (8) and $z^T \mathcal{P}_{\delta u}(\xi(\theta_0), \theta_0, 0) y \neq 0$.*

Remark 2. *Condition (8) is also a necessary condition of Theorem 1 for the limit cycle $(x_\delta(t), \theta_\delta(t))$ to exist (see Theorem 2).*

Remark 3. *The convergence guaranteed by Theorem 1 is of order δ by Theorem 2, see formula (48).*

IV. A Step-by-step Guide and Example

The following example of time-invariant ESC (3)-(4) will be used to illustrate the general guidelines

$$\dot{x}_1 = \gamma\left(-\frac{1}{r}x_2 + x_1\left\{(\theta + Mx_1 - \theta^*)^2 - x_1^2 - x_2^2 + R^2\right\}\right), \tag{10}$$

$$\dot{x}_2 = \gamma\left(r(x_1 - a(\theta)) + x_2\left\{(\theta + Mx_1 - \theta^*)^2 - x_1^2 - x_2^2 + R^2\right\}\right) \tag{11}$$

$$\begin{aligned} y_o &= x_1 \\ \dot{\theta} &= -\delta x_1^3 \end{aligned} \tag{12}$$

where $a(\theta) = -\frac{M}{M^2-1}(\theta - \theta^*)$, $r = \sqrt{1 - M^2}$, $M < 1$ is a positive constant, $\delta \in \mathbb{R}_+$ is a small parameter, and $\gamma \in \mathbb{R}_+$ determines the speed of the system. For this analysis, we set $\gamma = 1$; other values of γ will be considered in Section V. The system of differential equations (10)-(11) is typically used as a benchmark in problems where the closed form of a limit cycle is required, see e.g., [27, §2.4]. For simplifying the analysis, we follow the procedure in [6], where we neglect the filters in the detector and consider only $J(x) = x_1^2$ as our objective function[1]. Also, we consider a state-dependent dither signal $d(x, \theta) = x_1$ in this example. The multiplication of the cost function $J(x)$ with the dither signal $d(x, \theta)$ as in (4) results in x_1^3 in equation (12).

We first show that at $\delta = 0$, the Poincaré map $(x_2, \theta) \mapsto \mathcal{P}(x_2, \theta, \delta)$ of (10)-(12) induced by the cross-section $S = \{x \in \mathbb{R} : x_1 = 0, x_2 > 0\}$, exhibits a family of fixed points.

A. Families of Fixed Points at $\delta = 0$

Let $X_0(t) = [X_1(t), \; X_2(t), \; X_3(t)]^\top$ denote one solution of (10)-(12) at $\delta = 0$, which is given by

$$X_1(t) = \frac{1}{r}\sqrt{R^2 - \frac{(\theta - \theta^*)^2}{M^2 - 1}} \sin(t) + a(\theta), \tag{13}$$

$$X_2(t) = -\sqrt{R^2 - \frac{(\theta - \theta^*)^2}{M^2 - 1}} \cos(t), \tag{14}$$

$$X_3(t) = \theta_0, \tag{15}$$

where θ_0 is a constant. It can be easily noticed from (13)-(14) that for different initial conditions, i.e., different values of θ, the Poincaré map $(x_2, \theta) \mapsto \mathcal{P}(x_2, \theta, 0)$ has different fixed points $x_2 = \xi(\theta)$ on the cross-section $x_1 = 0, x_2 > 0$, as shown in Fig. 2. The "size" of the limit cycle of the system (10)-(11) is minimum at $\theta = \theta^*$, and we will now use Theorem 1 to show that the closed-loop system (10)-(12) converges in a neighborhood of this specific limit cycle for all $\delta > 0$ sufficiently close to zero.

[1] We have performed similar analysis to prove the minimization of $J(x) = x_1^2 + x_2^2$, but computations are too long to present in a manuscript.

$$\begin{bmatrix} X_{1_{\delta t}} \\ X_{2_{\delta t}} \\ X_{3_{\delta t}} \end{bmatrix} = \underbrace{\begin{bmatrix} -r^2(X_1-a)^2+R^2-\frac{(\theta-\theta^*)^2}{M^2-1}-X_2^2-2r^2X_1(X_1-a) & -\frac{1}{r}-2X_1X_2 & 2(X_1-a)MX_1-2\frac{(\theta-\theta^*)}{M^2-1}X_1 \\ r-2r^2X_2(X_1-a) & -r^2(X_1-a)^2+R^2-\frac{(\theta-\theta^*)^2}{M^2-1}-3X_2^2 & r\frac{M}{M^2-1}+2X_2(X_1-a)M-\frac{2(\theta-\theta^*)}{M^2-1}X_2 \\ 0 & 0 & 0 \end{bmatrix}}_{f_{(x_1,x_2,\theta)}(X_0(t,\theta))} \begin{bmatrix} X_{1\delta} \\ X_{2\delta} \\ X_{3\delta} \end{bmatrix} + \underbrace{\begin{bmatrix} 0 \\ 0 \\ -X_1^3 \end{bmatrix}}_{f_\delta(X_0(t,\theta))} \quad (16)$$

B. Analytic Stability Proof

In this section, we first compute the terms in Theorem 1 and then use them to prove the closed-loop system (10)-(12) has an asymptotically stable limit cycle. Let $X(t, x_1, x_2, \theta, \delta)$ denote the general solution of (10)-(12). Then $\mathcal{P}(x_2, \theta, \delta)$ will be given by the last two components of $X(2\pi, 0, x_2, \theta, \delta)$, i.e.

$$\mathcal{P}(x_2, \theta, \delta) = \begin{pmatrix} X_2(2\pi, 0, x_2, \theta, \delta) \\ X_3(2\pi, 0, x_2, \theta, \delta) \end{pmatrix}.$$

The entire analytic stability proof involves the computation of 1) $\mathcal{P}_\delta(\xi(\theta), \theta, 0)$); 2) Eigenvectors of $\mathcal{P}_{(x_2,\theta)}(\xi(\theta^*), \theta^*, 0)$; 3) $(\mathcal{P}_\delta)_{(x_2,\theta)}(\xi(\theta^*), \theta^*, 0)$ and, 4) Verification of conditions in Theorem 1.

1) Computation of $\mathcal{P}_\delta(\xi(\theta), \theta, 0)$: We have

$$\mathcal{P}_\delta(x_2, \theta, \delta) = \begin{pmatrix} (X_2)_\delta(2\pi, 0, x_2, \theta, \delta) \\ (X_3)_\delta(2\pi, 0, x_2, \theta, \delta) \end{pmatrix}. \quad (17)$$

In order to compute $X_\delta(t, 0, \xi(\theta), \theta, \delta)$, we substitute $X(t, x_1, x_2, \theta, \delta)$ for $(x_1, x_2, \theta)^\top$ in (10)-(12), differentiate (10)-(12) with respect to δ, and then substitute $\delta = 0$ to get

$$\begin{aligned} &X_{\delta t}(t, 0, x_2, \theta, 0) \\ &\quad = f_{(x_1,x_2,\theta)}(X(t, 0, x_2, \theta, 0)X_\delta(t, 0, x_2, \theta, 0) \\ &\quad + f_\delta(X(t, 0, x_2, \theta, 0)), \end{aligned} \quad (18)$$

For the example (10)-(12), (18) computes as (16). Plugging $(x_1, x_2, \theta) = (0, \xi(\theta), \theta)$ in $X(t, x_1, x_2, \theta, \delta)$ and denoting

$$X_0(t, \theta) = X(t, 0, \xi(\theta), \theta, 0),$$

equation (18) can be compactly written as

$$\dot{\eta} = f_{(x_1,x_2,\theta)}(X_0(t, \theta))\eta + f_\delta(X_0(t, \theta)), \quad (19)$$

where $\eta(t) = X_\delta(t, 0, \xi(\theta), \theta, 0)$. To solve (19) for η, we will use the variations of constants formula, which says that

$$\eta(t) = Y(t, \theta)\eta(0) + Y(t, \theta)\int_0^t Y(-s, \theta) f_\delta(X_0(s, \theta)) ds, \quad (20)$$

where $Y(t, \theta)$ is the fundamental matrix solution of the homogeneous equation

$$\dot{\eta} = f_{(x_1,x_2,\theta)}(X_0(t, \theta))\eta \quad (21)$$

with the initial condition $Y(0, \theta) = I_3 = Y^{-1}(0, \theta)$. Since we need to solve (19) in the neighborhood of $\theta = \theta^*$ only, we split $f_{(x_1,x_2,\theta)}(\cdot)$ to rewrite (21) as

$$\dot{\eta} = \{ \underbrace{A(t) + (\theta - \theta^*)B(t, \theta - \theta^*)}_{f_{(x_1,x_2,\theta)}(\cdot)} \}\eta. \quad (22)$$

For the example (10)-(12), by combining (13)-(15), we obtain

$$A(t) = \begin{bmatrix} -2R^2\sin^2(t) & \frac{R^2\sin(2t)-1}{\sqrt{1-M^2}} & \frac{2MR^2\sin^2(t)}{1-M^2} \\ \sqrt{1-M^2}(1+R^2\sin(2t) & -2R^2\cos^2(t) & \frac{-M-MR^2\sin(2t)}{\sqrt{1-M^2}} \\ 0 & 0 & 0 \end{bmatrix} \quad (23)$$

and $B(t, (\theta - \theta^*))$ is given by (55). Expanding $Y(t, \theta)$ in Taylor series about $\theta = \theta^*$ up to first order, we get

$$Y(t, \theta) = \underbrace{Y(t, \theta^*) + (\theta - \theta^*)Y_\theta(t, \theta^*)}_{\widetilde{Y}(t,\theta)} + o(\theta - \theta^*), \quad (24)$$

where $Y(t, \theta^*)$ is the matrix solution of

$$\dot{\eta} = A(t)\eta \quad (25)$$

with the initial condition $Y(0, \theta^*) = I_3$. The matrix-solution $Y(t, \theta^*)$ of the reduced linear system (25) computes as

$$Y(t, \theta^*) = \begin{bmatrix} \cos(t) & -\frac{e^{-2R^2t}\sin(t)}{\sqrt{1-M^2}} & -\frac{M}{M^2-1}+\frac{M\cos(t)}{M^2-1} \\ \sqrt{1-M^2}\sin(t) & e^{-2R^2t}\cos(t) & \frac{M\sqrt{1-M^2}\sin(t)}{M^2-1} \\ 0 & 0 & 1 \end{bmatrix}. \quad (26)$$

To find $Y_\theta(t, \theta^*)$, we plug the matrix solution $Y(t, \theta)$ into (22) for η and differentiate (22) with respect to θ at $\theta = \theta^*$ to get

$$Y_{t\theta} = A(t)Y_\theta + B(t, 0)Y,$$

where Y stands for $Y(t, \theta^*)$. Since $Y(0, \theta) = I_3$ for all θ, we have $Y_\theta(0, \theta^*) = 0_3$, so we can use the variations of constants formula to get

$$Y_\theta(t, \theta^*) = Y(t, \theta^*)\int_0^t Y(-s, \theta^*)B(s, 0)Y(s, \theta^*) \mathrm{d}s, \quad (27)$$

which was computed using Wolfram Mathematica. The expression for $Y_\theta(t, \theta^*)$ is very lengthy, and therefore we refer the readers to the supplementary Mathematica notebook file, which is available for download. Using the closed form expressions for $Y(t, \theta^*)$ and $Y_\theta(t, \theta^*)$ from (26) and (27), we can compute $\widetilde{Y}(t, \theta)$ in (24). Therefore, we can use the variation of constants formula (20) with the initial condition $X_\delta(0, 0, \xi(\theta), 0) = 0_3$ to compute $X_\delta(t, 0, \xi(\theta), 0)$ as

$$\begin{aligned} X_\delta(t, 0, \xi(\theta), 0) = \widetilde{Y}(t, \theta)\int_0^t \widetilde{Y}(-s, \theta) f_\delta(X_0(s, \theta)) \mathrm{d}s \\ + o(\theta - \theta^*). \end{aligned} \quad (28)$$

Substituting $t = 2\pi$ in (28) and using Wolfram Mathematica to compute the integral (28), we finally obtain an expression for $\mathcal{P}_\delta(\xi(\theta), \theta)$ as

$$\begin{aligned} \mathcal{P}_\delta(\xi(\theta), \theta) = \begin{bmatrix} * \\ \frac{M\pi\{-3(-1+M^2)R^2+(3+2M^2)(\theta-\theta^*)^2\}(\theta-\theta^*)}{(-1+M^2)^3} \end{bmatrix} \\ + o(\theta - \theta^*). \end{aligned} \quad (29)$$

2) Computation of Eigenvectors of $\mathcal{P}_{(x_2,\theta)}(\xi(\theta^*), \theta^*, 0)$: In order to verify conditions (8), (9) of Theorem 1, we need to find the eigenvectors z, y of $\mathcal{P}_{(x_2,\theta)}(\xi(\theta^*), \theta^*, 0)^\top$, $\mathcal{P}_{(x_2,\theta)}(\xi(\theta^*), \theta^*, 0)$, respectively, that correspond to eigenvalue 1. We have

$$\begin{aligned} &\mathcal{P}_{(x_2,\theta)}(\xi(\theta^*), \theta^*, 0) = \\ &\qquad \begin{bmatrix} (X_2)_{x_2} & (X_2)_\theta \\ (X_3)_{x_2} & (X_3)_\theta \end{bmatrix} \Big(2\pi, 0, \xi(\theta^*), \theta^*, 0\Big). \end{aligned} \quad (30)$$

To compute the first column terms of $\mathcal{P}_{(x_2,\theta)}(\xi(\theta^*), \theta^*, 0)$ in (30), we substitute $X(t, x_1, x_2, \theta, \delta)$ for $(x_1, x_2, \theta)^\top$ in (10)-(12), set $\delta = 0$, and then differentiate (10)-(12) with respect to x_2 to obtain

$$X_{x_2 t}(t, 0, \xi(\theta), \theta, 0) = f_{(x_1,x_2,\theta)}(X_0(t, \theta))X_{x_2}(t, 0, \xi(\theta), \theta, 0),$$

where $f_{(x_1,x_2,\theta)}(x_0(t, \theta))$ is the same matrix as in (16). Since $f_{(x_1,x_2,\theta)}(X_0(t, \theta^*)) = A(t)$ from (22), we can use the fundamental matrix solution $Y(t,\theta^*)$ that we found for (21) in (26) along with the initial condition $X_{x_2}(0,0,\xi(\theta^*),\theta^*,0) = (0,\ 1,\ 0)^\top$ to obtain

$$X_{x_2}(2\pi,0,\xi(\theta^*),\theta^*,0) = Y(2\pi,\theta^*)X_{x_2}(0,0,\xi(\theta^*),\theta^*,0)$$
$$= Y(2\pi,\theta^*)\begin{bmatrix}0\\1\\0\end{bmatrix} \underline{\underline{\text{for (10)–(12)}}} \begin{bmatrix}0\\e^{-4\pi R^2}\\0\end{bmatrix}. \quad (31)$$

Next, to compute the second column terms of $\mathcal{P}_{(x_2,\theta)}(\xi(\theta^*),\theta^*,0)$ in (30), we follow the same procedure, where we differentiate (10)-(12) with respect to θ and set $\delta = 0$ to get

$$X_{\theta t}(t,0,\xi(\theta),\theta,0) = f_{(x_1,x_2,\theta)}(X_0(t,\theta))X_\theta(t,0,\xi(\theta),\theta,0). \quad (32)$$

Similar to (31), we can compute the solution of (32) using the initial condition $X_\theta(0,0,\xi(\theta),\theta,0) = (0,\ 0,\ 1)^\top$ to get

$$X_\theta(2\pi,0,\xi(\theta^*),\theta^*,0) = Y(2\pi,\theta^*)X_\theta(0,0,\xi(\theta^*),\theta^*,0)$$
$$= Y(2\pi,\theta^*)\begin{bmatrix}0\\0\\1\end{bmatrix} \underline{\underline{\text{for (10)–(12)}}} \begin{bmatrix}0\\0\\1\end{bmatrix}. \quad (33)$$

Plugging in (31) and (33) to (30), we get the following expression for $\mathcal{P}_{(x_2,\theta)}(\xi(\theta^*),\theta^*,0)$ of example (10)-(12):

$$\mathcal{P}_{(x_2,\theta)}(\xi(\theta^*),\theta^*,0) = \begin{bmatrix}e^{-4\pi R^2} & 0\\ 0 & 1\end{bmatrix}. \quad (34)$$

From (34), it can be seen that $\mathcal{P}_{(x_2,\theta)}(\cdot) = \mathcal{P}^\top_{(x_2,\theta)}(\cdot)$, which implies that the eigenvectors z and y are equal and given by

$$z = y = \begin{bmatrix}0\\1\end{bmatrix}. \quad (35)$$

Note that (35) holds for all values of θ. Furthermore, the eigenvalue ρ_2 of $\mathcal{P}_{(x_2,\theta)}(\xi(\theta^*),\theta^*,0)$ is in the interval $(-1,1)$ because, from (34), ρ_2 computes as

$$\rho_2 = e^{-4\pi R^2}. \quad (36)$$

3) Computation of $(\mathcal{P}_\delta)_{(x_2,\theta)}(\xi(\theta^*),\theta^*,0)$: In order to verify (9) of Theorem 1, we need to compute $(\mathcal{P}_\delta)_{(x_2,\theta)}(\xi(\theta^*),\theta^*,0)$, which is

$$(\mathcal{P}_\delta)_{(x_2,\theta)}(\xi(\theta^*),\theta^*,0) = \begin{bmatrix}(X_2)_{\delta x_2} & (X_2)_{\delta\theta}\\ (X_3)_{\delta x_2} & (X_3)_{\delta\theta}\end{bmatrix}\Big(2\pi,0,\xi(\theta^*),\theta^*,0\Big). \quad (37)$$

To compute the first column terms of (37), we differentiate (18) with respect to x_2 to get

$$X_{x_2\delta t}(t,0,\xi(\theta^*),\theta^*,0) = A(t)X_{x_2\delta}(t,0,\xi(\theta^*),\theta^*,0) + H_1(t), \quad (38)$$

where $A(t)$ is the same matrix as in (22). The computation of $H_1(t)$ at $\theta = \theta^*$ for the example (10)-(12) is executed in (56). In order to obtain the general solution of (38), we use the variations of constants formula with the initial condition $X_{x_2\delta}(0,0,\xi(\theta^*),\theta^*,0) = (0,\ 0,\ 0)^\top$ to get

$$X_{x_2\delta}(2\pi,0,\xi(\theta^*),\theta^*,0) = Y(2\pi,\theta^*)\int_0^{2\pi} Y(-s,\theta^*)H_1(s)\mathrm{d}s$$
$$\underline{\underline{\text{for (10)–(12)}}} \begin{bmatrix}*\\ *\\ \frac{3(6-6e^{-4\pi R^2})R^2}{(1-M^2)^{3/2}(9+40R^4+16R^8)}\end{bmatrix} \quad (39)$$

Similarly, to compute the second column terms of (37), we differentiate (18) with respect to θ and get

$$X_{\theta\delta t}(t,0,\xi(\theta^*),\theta^*,0) = A(t)X_{\theta\delta}(t,0,\xi(\theta^*),\theta^*,0) + H_2(t). \quad (40)$$

For the example (10)-(12), the computation of H_2 at $\theta = \theta^*$ is mentioned in (57). In order to obtain the general solution of (40) with the initial condition $X_{\theta\delta}(0,0,\xi(\theta^*),\theta^*,0) = (0,\ 0,\ 0)^\top$, we use variations of constants formula, giving

$$X_{\theta\delta}(2\pi,0,\xi(\theta^*),\theta^*,0) = Y(2\pi,\theta^*)\int_0^{2\pi} Y(-s,\theta^*)H_2(s)\mathrm{d}s$$
$$\underline{\underline{\text{for (10)–(12)}}} \begin{bmatrix}*\\ *\\ -\frac{3M\pi R^2}{(M^2-1)^2}\end{bmatrix}. \quad (41)$$

Plugging in the last two rows of (39) and (41) in (37), the derivative $(\mathcal{P}_\delta)_{(x_2,\theta)}(\xi(\theta^*),\theta^*,0)$ computes for (10)-(12) as

$$(\mathcal{P}_\delta)_{(x_2,\theta)}(\xi(\theta^*),\theta^*,0) = \begin{bmatrix}* & *\\ \frac{3(6-6e^{-4\pi R^2})R^2}{(1-M^2)^{3/2}(9+40R^4+16R^8)} & -\frac{(3M\pi R^2)}{(M^2-1)^2}\end{bmatrix}. \quad (42)$$

4) Verification of Conditions in Theorem 1 for the Example (10)-(12): In order to verify (8) of Theorem 1, we use (29) and (35) to get

$$z^\top P_\delta(\xi(\theta),\theta,0) = \frac{M\pi\{-3(-1+M^2)R^2+(3+2M^2)(\theta-\theta^*)^2\}(\theta-\theta^*)}{(-1+M^2)^3},$$

which is zero only at $\theta = \theta^*$. Next, we use (35) and (42) in (9) to get

$$z^\top(P_\delta)_{(x_2,\theta)}(\xi(\theta^*),\theta^*,0)y = -\frac{3M\pi R^2}{(M^2-1)^2}, \quad (43)$$

which is less than zero. This verifies (9) of Theorem 1. Next, (7) of Theorem 1 holds by (36).

V. Simulation Results

First, the system (10)-(11), along with time-invariant ESC dynamics (12), was simulated with two different initial conditions: (i) $[x_1(0), x_2(0), \theta(0)] = [2, 0, 1]$ and (ii) $[x_1(0), x_2(0), \theta(0)] = [2, 0, 5]$. We chose $\gamma = 1$, $R = 1$ in (10)-(11). The time-invariant ESC parameters were selected as $\delta = 0.12, M = 0.015$. The optimum in this simulation was $\theta^* = 3.0$. From Fig. 3, it can be seen that our time-invariant ESC tunes θ to $\theta^* = 3$, starting from two different initial conditions of θ. Also, it can be seen from Fig. 4 that the time-invariant ESC reduces the amplitude of the states x_1, x_2, which have a peak-to-peak amplitude that tends to $R = 1$.

Next, we compare the performance of time-invariant ESC with time-based ESC for different speeds of the system determined by γ in (10)-(11). For time-based ESC, we tuned its parameters for a particular γ, which resulted in stable adaptation of θ. In particular, the parameters $a = 0.015$, $\omega = 0.1$ rad/s, $\delta = 0.03$ were selected for the time-based ESC. Similarly, for time-invariant ESC, the parameters $\delta = 0.03$, $M = 0.015$ were selected. As evident from Fig. 5, the time-invariant ESC is less sensitive to changes in time-scale of the plant compared to the time-based ESC. However, we remark here that if a plant slows down sufficiently, δ needs to be re-tuned in order to maintain time-scale separation between the plant and the ESC dynamics.

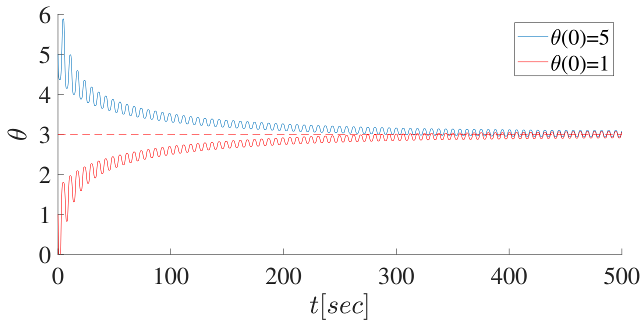

Fig. 3: Time-invariant ESC adaptation of θ from different initial conditions of θ. The horizontal dashed line represents the value of θ^*.

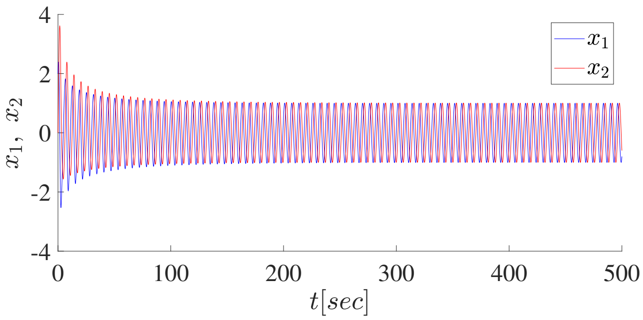

Fig. 4: Plot of states x_1, x_2 of the system (10)-(11) starting from initial conditions $[x_1(0), x_2(0)] = [2, 0]$ during time-invariant ESC adaptation.

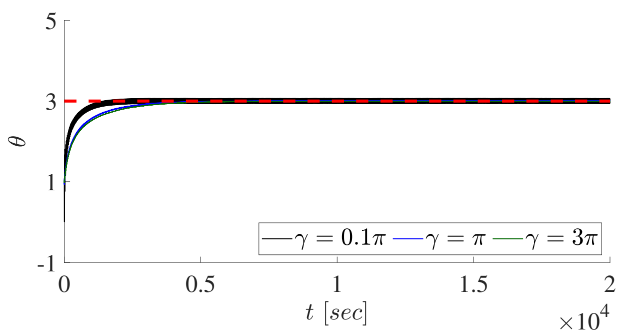

(a) Time-invariant ESC adaptation of θ for different values of γ.

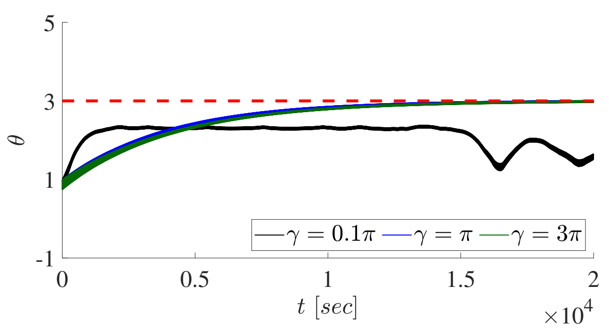

(b) Time-based ESC adaptation of θ for different values of γ.

Fig. 5: Performance comparison between time-invariant and time-based ESC for different speeds of the system. Figs. 5a, 5b shows the time-invariant and time-based ESC adaptation of θ to $\theta^* = 3$ for different values of γ without changing the ESC parameters. It can be seen that for slower plant speeds, the time-based ESC adaptation of θ becomes unstable for $\gamma = 0.1\pi$.

VI. Discussion and Conclusion

We presented time-invariant ESC for nonlinear autonomous systems with limit cycles. The general formulation of our ESC scheme uses a measurement of the state vector x of the system (3)-(4). However, the knowledge of a single component of x can be sufficient, as shown in our example. No other information or knowledge of the system is needed for our approach. This can be contrasted with [29], where the authors assume explicit relation between the plant dynamics and the unknown parameters and consequently use estimation techniques to achieve extremum seeking.

For this time-invariant ESC, we present a method for proving asymptotic stability of the limit cycle for the closed loop system, which is based on perturbation theory for maps. In particular, we stated the necessary and sufficient conditions concerning the convergence of the solutions of (3)-(4) to a limit cycle of (3) for any specified value of $\theta = \theta_0$. Condition (7) assumes asymptotic stability of each individual limit cycle of the 1-parameter family of cycles of the plant system. This condition is natural, because our approach is non-invasive and cannot reverse the stability of limit cycles. Our control rule only tunes the parameter to ensure that the limit cycle of minimal amplitude is attained. Every example that we have considered suggests that condition (8) is always satisfied only at $\theta = \theta^*$ and not for any other values of θ. However, we do not have a mathematical proof yet for this fact. Therefore, at present, our result requires verifying condition (8) for a given plant. Whether this requirement can be dropped, or there exist a counter-example showing that it cannot be dropped, is an interesting mathematical question that we will address in the future. Finally, the stability condition (7) in Theorem 1 alone is not sufficient to establish asymptotic stability of the full system (3)-(4), because (7) does not consider the dynamics of the time-invariant ESC (4). Therefore, an additional condition (9) is required to ensure asymptotic stability of the full system.

The step-by-step guide of Section IV can be applied to any general system (3)-(4) once the limit cycle of (3) is computable explicitly. If the limit cycle of (3) cannot be computed explicitly, applying the guide with an approximation of this limit cycle will produce the correct conclusions as long as the derivative (9) converges to a non-zero value (*non-degeneracy condition*) as the approximation error decreases. The fact that it is sufficient to verify the conditions of Theorem 1 for an approximation of the limit cycle of (3) when the non-degeneracy condition holds can be rigorously justified over the methods of the Implicit Function Theorem. Verification of the non-degeneracy condition can be done numerically.

We discovered that having $a \neq 0$ (that follows from (43) because $M \neq 0$) plays a crucial role in our example, as it dismantles the symmetry of the limit cycle of (10)-(11), which is required for the validity of condition (9) in Theorem 1. This is due to the fact that the main ingredients $z^\top \mathcal{P}_\delta(\xi(\theta^*), \theta^*, 0)$ and $z^\top \mathcal{P}_{\delta u}(\xi(\theta^*), \theta^*, 0)$ of this theorem represent an analogue of averaging functions and its derivative (see [20, Section 4]), so it is natural to expect that the averaging of a symmetric function returns zero, violating condition (49). In particular, we expect that the non-degeneracy condition of the previous paragraph will hold when the limit cycle of (3) is non-symmetric in a proper way.

Though it is not obvious how generalizing equations (10)-(11) can lead to explicitly computable terms of Theorem 1, generalizing the cost function (12) is a reasonable task that will be based on an analysis of abstract integrals (obtained along the lines of Section IV). Moreover, our preliminary analysis indicates that replacing (12) with a polynomial function would lead to explicitly computable integrals and a closed form (though long) of condition (43). Analysis of the above-mentioned integrals is an interesting mathematical task, but it is outside of the focused scope of this Technical Note.

Appendix

In what follows, we present a proof of Theorem 1, which is a combination of Theorems 2 and 3 stated in this section. We first state a lemma with its proof, which will be used in the proof of Theorem 2. We then present several long expressions from our analysis in Section IV.

Lemma 1. *If*

$$z^T y = 1, \quad \text{and} \quad \tilde{z}^T \tilde{y} = I_{n-1}, \tag{44}$$

then any $\zeta \in \mathbb{R}^n$ can be decomposed as

$$\zeta = y z^T \zeta + \tilde{y} \tilde{z}^T \zeta. \tag{45}$$

Furthermore, (44) ensures that y and the $(n-1)$-dimensional hyperplane $\mathrm{lin}(\tilde{y})$ formed by vectors $\tilde{y}$ are linearly independent and

$$\pi \zeta = y z^T \zeta, \tag{46}$$

where $\pi\zeta$ is the projection of ζ on y along $\mathrm{lin}(\tilde{y})$.

Proof. First, observe that since (y, z) and $(\tilde{y}, \tilde{z})$ are the eigenvectors that correspond to eigenvalues $\rho_1 = 1$ and $\rho_2 \neq 1$ of some matrices A and A^T, then

$$\tilde{z}^T y = z^T \tilde{y} = 0. \tag{47}$$

Indeed, from $A^T \tilde{z} = \tilde{z} \rho_2$ we have $\tilde{z}^T A = \rho_2^T \tilde{z}^T$. Therefore, $\tilde{z}^T A y = \rho_2^T \tilde{z}^T y$, which implies $\tilde{z}^T y = \rho_2^T \tilde{z}^T y$, and so $\tilde{z}^T y = 0$. The second equality follows by a similar argument.

Formulas (44) and (47) imply that y and $\mathrm{lin}(\tilde{y})$ are linearly independent and so $\pi\zeta$ is defined. By the definition of $\pi\zeta$, we have $\zeta - \pi\zeta \in \mathrm{lin}(\tilde{y})$ and so, by (47), $z^T(\zeta - \pi\zeta) = 0$. Let $\pi\zeta = y\lambda$, where $\lambda \in \mathbb{R}$. Using (44),

$$z^T \zeta = z^T \pi \zeta = z^T y \lambda = \lambda,$$

which implies (46).

Similarly, let $\tilde{\pi}\zeta$ be the projection of ζ on the hyperplane formed by vector $\tilde{y}$ along y. Then, $\tilde{z}^T(\zeta - \tilde{\pi}\zeta) = 0$. Since $\tilde{\pi}\zeta \in \mathrm{lin}(\tilde{y})$, there exists $\tilde{\lambda} \in \mathbb{R}^{n-1}$ such that $\tilde{\pi}\zeta = \tilde{y}\tilde{\lambda}$. Arguing as above, we get

$$\tilde{\pi}\zeta = \tilde{y} \tilde{z}^T \zeta.$$

Therefore, (45) coincides with the rule of the sum of vectors, i.e., $\zeta = \pi\zeta + \tilde{\pi}\zeta$. □

Theorem 2. ***(Necessary and Sufficient Condition for Existence of Limit Cycles) — Necessity Part:*** *Let the Poincaré map $\mathcal{P}$ be a C^3 function, and assume that $z^\top y \neq 0$. If, for each $\delta \in \mathbb{R}$, $u \mapsto \mathcal{P}(u, \delta)$ admits a fixed point $u_\delta \in \mathbb{R}^n$ such that*

$$\|u_\delta - u_0\| \leq N\delta, \quad u_0 = \xi(s_0), \tag{48}$$

for some $N > 0$, $s_0 \in \mathbb{R}$, and for all $|\delta|$ sufficiently small, then (8) holds.

Sufficiency Part: *In addition to (8), assume that*

$$z^\top \mathcal{P}_{\delta u}(u_0, v_0, 0) y \neq 0 \tag{49}$$

and (6) hold. Assume further that the eigenvector z does not depend on s_0, i.e.

$$z^T(\mathcal{P}_u(\xi(s), 0) - I) = 0, \quad \text{for all } s \in \mathbb{R}. \tag{50}$$

Then, for all $|\delta|$ sufficiently small, the Poincaré map $u \mapsto \mathcal{P}(u, \delta)$ does indeed have a fixed point u_δ that satisfies (48) for some $N > 0$ and for all $|\delta|$ sufficiently small.

Proof. **Necessity part:** We expand $\mathcal{P}(u, \delta)$ up to first order as

$$\mathcal{P}(u, \delta) = \mathcal{P}(u, 0) + \delta P_\delta(u, \delta).$$

Therefore,

$$\frac{1}{\delta} z^T \Big[\mathcal{P}(u_\delta, 0) + \delta P_\delta(u_\delta, \delta) - u_\delta\Big] = 0. \tag{51}$$

Expanding $\mathcal{P}(u, 0)$ in Taylor Series up to first order about $u = u_0$, we can rewrite the latter equality as

$$\frac{z^T}{\delta}\Big[\mathcal{P}(u_0, 0) + \mathcal{P}_u(u_0, 0)(u_\delta - u_0) + \delta P_\delta(u_\delta, \delta) - u_\delta + o(u_\delta - u_0)\Big] = 0.$$

By the definition of z, we have $\mathcal{P}_u(u_0, 0)^T z = z$, whose transpose gives

$$z^T \mathcal{P}_u(u_0, 0) = z^T. \tag{52}$$

Using (52) and the fact that $\mathcal{P}(u_0, 0) = u_0$, we conclude

$$z^T \mathcal{P}_\delta(u_\delta, \delta) + \frac{1}{\delta} o(u_\delta - u_0) = 0,$$

which implies (8) due to (48).

Sufficiency part: Introduce

$$F(u, \delta) = \mathcal{P}(u, \delta) - u. \tag{53}$$

To obtain the required statement from [20, Theorem 1] we need to prove that

(i) $\pi F_u(u_0, 0)\mathbb{R}^n = F_u(u_0, 0)\pi\mathbb{R}^n$,
(ii) matrix $F_u(u_0, 0)$ is invertible on $(I - \pi)\mathbb{R}^n$,
(iii) $\pi F_\delta(u_0, 0) = 0$,
(iv) matrix $\pi F_{uu}(u_0, 0)h$ vanishes on $\pi\mathbb{R}^n$ for any $h \in \mathbb{R}^n$,
(v) matrix $\pi F_{\delta u}(u_0, 0)$ is invertible on $\pi\mathbb{R}^n$.

Indeed, (i) holds because $F_u(u_0, 0)y = z^T F_u(u_0, 0) = 0$ by the definition of y and z. By Lemma 1,

$$(I - \pi)\zeta = \tilde{y} \tilde{z}^T \zeta.$$

Therefore, (ii) holds by (6). Property (iii) coincides with (8). By differentiating (50) at $s = s_0$, we get

$$z^T P_{uu}(u_0, 0) y = 0,$$

which implies (iv). Finally, (v) follows from (49). The conclusion now follows from Theorem 1 and Remark 2 of [20]. The value N can be taken as e.g. $N = 2\|w_0\|$, where w_0 is that given by [20, Theorem 1]. □

$$B(t,\theta-\theta^{*})=\begin{bmatrix} \frac{2\sin(t)\{M\sqrt{1\text{-}M^2}\sqrt{R^2\text{-}\frac{(\theta\text{-}\theta^*)^2}{M^2\text{-}1}}+(\theta\text{-}\theta^*)\sin(t)\}}{M^2\text{-}1} & \frac{2\cos(t)\{M\sqrt{1\text{-}M^2}\sqrt{R^2\text{-}\frac{(\theta\text{-}\theta^*)^2}{M^2\text{-}1}}+(\theta\text{-}\theta^*)\sin(t)\}}{(1\text{-}M^2)^{3/2}} & \frac{3M(\theta\text{-}\theta^*)\text{-}M(\theta\text{-}\theta^*)\cos(2t)+2\sqrt{1\text{-}M^2}(1+M^2)\sqrt{R^2\text{-}\frac{(\theta\text{-}\theta^*)^2}{M^2\text{-}1}}\sin(t)}{(M^2\text{-}1)^2} \\ \frac{(\theta-\theta^*)\sin(2t)}{\sqrt{1\text{-}M^2}} & \frac{2(\theta\text{-}\theta^*)\cos^2(t)}{M^2\text{-}1} & \text{-}\frac{2\cos(t)\{\sqrt{1\text{-}M^2}\sqrt{R^2\text{-}\frac{(\theta\text{-}\theta^*)^2}{M^2\text{-}1}}+M(\theta\text{-}\theta^*)\sin(t)\}}{(1\text{-}M^2)^{3/2}} \\ 0 & 0 & 0 \end{bmatrix} \tag{55}$$

$$H_1(t)=\begin{bmatrix} x_{1_\delta}\{\text{-}2r^2(x_1\text{-}a)(x_{1_{x_2}}+\frac{M}{M^2\text{-}1}\theta_{x_2})\text{-}2x_2x_{2_{x_2}}\}+x_{1_{x_2}}\{\text{-}2r^2(x_1\text{-}a)(x_{1_\delta}+\frac{M}{M^2\text{-}1}\theta_\delta)\text{-}2x_2x_{2_\delta}\} - 2r^2x_1(x_{1_{x_2}}+\frac{M}{M^2\text{-}1}\theta_{x_2})(x_{1_\delta}+\frac{M}{M^2\text{-}1}\theta_\delta)\text{-}2\theta_{x_2}\theta_\delta x_1\text{-}2x_{2_{x_2}}x_{2_\delta}x_1 \\ x_{2_\delta}\{\text{-}2r^2(x_1\text{-}a)(x_{1_{x_2}}+\frac{M}{M^2\text{-}1}\theta_{x_2})\text{-}2x_2x_{2_{x_2}}\}+x_{2_{x_2}}\{\text{-}2r^2(x_1\text{-}a)(x_{1_\delta}+\frac{M}{M^2\text{-}1}\theta_\delta)\text{-}2x_2x_{2_\delta}\} + x_2\{\text{-}2r^2(x_{1_{x_2}}+\frac{M}{M^2\text{-}1}\theta_{x_2})(x_{1\delta}+\frac{M}{M^2\text{-}1}\theta_\delta)\text{-}\frac{2\theta_{x_2}\theta_\delta}{M^2\text{-}1}\text{-}2x_{2_{x_2}}x_{2_\delta} \\ -3x_1^2x_{1_{x_2}} \end{bmatrix} \tag{56}$$

$$H_2(t)=\begin{bmatrix} x_{1_\delta}\{\text{-}2r^2(x_1\text{-}a)(x_{1_\theta}+\frac{M}{M^2\text{-}1}\theta_\theta)\text{-}2x_2x_{2_\theta}\}+x_{1_\theta}\{\text{-}2r^2(x_1\text{-}a)(x_{1_\delta}+\frac{M}{M^2\text{-}1}\theta_\delta)\text{-}2x_2x_{2_\delta}\} - 2r^2x_1(x_{1_\theta}+\frac{M}{M^2\text{-}1}\theta_\theta)(x_{1_\delta}+\frac{M}{M^2\text{-}1}\theta_\delta)\text{-}2\theta_\theta\theta_\delta x_1\text{-}2x_{2_\theta}x_{2_\delta}x_1 \\ x_{2_\delta}\{\text{-}2r^2(x_1\text{-}a)(x_{1_\theta}+\frac{M}{M^2\text{-}1}\theta_\theta)\text{-}2x_2x_{2_\theta}\}+x_{2_\theta}\{\text{-}2r^2(x_1\text{-}a)(x_{1_\delta}+\frac{M}{M^2\text{-}1}\theta_\delta)\text{-}2x_2x_{2_\delta}\} + x_2\{\text{-}2r^2(x_{1_\theta}+\frac{M}{M^2\text{-}1}\theta_\theta)(x_{1\delta}+\frac{M}{M^2\text{-}1}\theta_\delta)\text{-}\frac{2\theta_\theta\theta_\delta}{M^2\text{-}1}\text{-}2x_{2_\theta}x_{2_\delta} \\ -3x_1^2x_{1_\theta} \end{bmatrix} \tag{57}$$

Theorem 3. ***(Sufficient Condition for Stability of Limit Cycles) —*** *Assume that sufficient conditions of Theorem 1 hold with*

$$z^\top y > 0, \tag{54}$$

and let u_δ be the fixed points satisfying (48). The fixed point u_δ is asymptotically stable, for all $\delta > 0$ sufficiently small, if (7) is satisfied, and if (49) holds in the stronger sense (9).

Proof. Let ρ_δ be the eigenvalue of $P_u(u_\delta, \delta)$ satisfying

$$\rho_\delta \to 1 \quad \text{as} \quad \delta \to 0.$$

Observe that $\lambda_\delta = \rho_\delta - 1$ is the eigenvalue of $F_u(u_\delta, \delta)$ for F given by (53). Thanks to (iv) of the proof of Theorem 2, the negativity of λ_δ for all $\delta > 0$ sufficiently small will follow from [20, Theorem 2], if the eigenvalue λ_* of the one-dimensional map $\pi F_{\delta u}(u_0, 0) : \pi\mathbb{R}^n \to \pi\mathbb{R}^n$ is negative. By (46), we have $\lambda_* = z^T F_{\delta u}(u_0, 0) y$ and so $\lambda_* < 0$ by (9). $\square$

Long Expressions — The equations for $B(t, \theta - \theta^*)$ in (22), $H_1(t)$ in (38) and $H_2(t)$ in (40) are given by (55), (56) and (57), respectively.

References

[1] S. Kumar, A. Mohammadi, N. Gans, and R. D. Gregg, "Automatic tuning of virtual constraint-based control algorithms for powered knee-ankle prostheses," in *IEEE Conf. on Control Tech. and App.*, Aug 2017, pp. 812–818.

[2] U. von Wagner, D. Hochlenert, and P. Hagedorn, "Minimal models for disk brake squeal," *Journal of Sound and Vibration*, vol. 302, no. 3, pp. 527–539, 2007.

[3] C. M. Denegri Jr, "Limit cycle oscillation flight test results of a fighter with external stores," *Journal of Aircraft*, vol. 37, no. 5, pp. 761–769, 2000.

[4] M. Krstić and H.-H. Wang, "Stability of extremum seeking feedback for general nonlinear dynamic systems," *Automatica*, vol. 36, no. 4, pp. 595–601, 2000.

[5] K. B. Ariyur and M. Krstic, *Real-time optimization by extremum-seeking control*. John Wiley & Sons, 2003.

[6] H. H. Wang and M. Krstić, "Extremum seeking for limit cycle minimization," *IEEE Trans. Autom. Control*, vol. 45, no. 12, pp. 2432–2437, 2000.

[7] M. Haring, N. Van De Wouw, and D. Nešić, "Extremum-seeking control for nonlinear systems with periodic steady-state outputs," *Automatica*, vol. 49, no. 6, pp. 1883–1891, 2013.

[8] S. Kumar *et al.*, "Extremum seeking control for model-free auto-tuning of powered prosthetic legs," *IEEE Trans. Control Syst. Technol.*, pp. 1–16, 2019.

[9] S. Kumar, M. R. Zwall, E. A. Bolívar-Nieto, R. D. Gregg, and N. Gans, "Extremum seeking control for stiffness auto-tuning of a quasi-passive ankle exoskeleton," *IEEE Robotics and Automation Letters*, vol. 5, no. 3, pp. 4604–4611, 2020.

[10] Y. Tan, D. Nešić, and I. Mareels, "On non-local stability properties of extremum seeking control," *Automatica*, vol. 42, no. 6, pp. 889–903, 2006.

[11] F. J. Diedrich and W. H. Warren Jr, "Why change gaits? dynamics of the walk-run transition." *Journal of Experimental Psychology: Human Perception and Performance*, vol. 21, no. 1, p. 183, 1995.

[12] S. Rezazadeh *et al.*, "A phase variable approach for improved rhythmic and non-rhythmic control of a powered knee-ankle prosthesis," *IEEE Access*, vol. 7, pp. 109 840–109 855, 2019.

[13] D. Quintero, D. J. Villarreal, D. J. Lambert, S. Kapp, and R. D. Gregg, "Continuous-phase control of a powered knee-ankle prosthesis: Amputee experiments across speeds and inclines," *IEEE Transactions on Robotics*, vol. 34, no. 3, pp. 686–701, June 2018.

[14] B. D. Anderson and A. Dehghani, "Challenges of adaptive control–past, permanent and future," *Annual Reviews in Control*, vol. 32, no. 2, pp. 123 – 135, 2008.

[15] A. Scheinker and M. Krstić, "Minimum-seeking for CLFs: Universal semiglobally stabilizing feedback under unknown control directions," *IEEE Trans. Autom. Control*, vol. 58, no. 5, pp. 1107–1122, 2012.

[16] A. Scheinker and D. Scheinker, "Bounded extremum seeking with discontinuous dithers," *Automatica*, vol. 69, pp. 250–257, 2016.

[17] A. Scheinker and M. Krstić, *Model-free stabilization by extremum seeking*. Springer, 2017.

[18] S. Kumar, A. Mohammadi, R. D. Gregg, and N. Gans, "Limit cycle minimization by time-invariant extremum seeking control," in *American Control Conference (ACC)*, 2019, pp. 2359–2365.

[19] Y. Zhang, O. Makarenkov, and N. Gans, "Extremum seeking control of a nonholonomic system with sensor constraints," *Automatica*, vol. 70, pp. 86–93, 2016.

[20] M. Kamenskii, O. Makarenkov, and P. Nistri, "An alternative approach to study bifurcation from a limit cycle in periodically perturbed autonomous systems," *Journal of Dynamics and Differential Equations*, vol. 23, no. 3, pp. 425–435, 2011.

[21] O. Makarenkov, "Existence and stability of limit cycles in the model of a planar passive biped walking down a slope," *Proceedings of the Royal Society A: Mathematical, Physical and Engineering Sciences*, vol. 476, no. 2233, p. 20190450, 2020.

[22] G. A. Leonov, "Pyragas stabilizability via delayed feedback with periodic control gain," *Systems & Control Letters*, vol. 69, pp. 34–37, 2014.

[23] A. Cetinkaya and T. Hayakawa, "A sampled-data approach to pyragas-type delayed feedback stabilization of periodic orbits," *IEEE Trans. Autom. Control*, vol. 64, no. 9, pp. 3748–3755, 2018.

[24] B. Fiedler, V. Flunkert, P. Hövel, and E. Schöll, "Delay stabilization of periodic orbits in coupled oscillator systems," *Philosophical Transactions of the Royal Society A: Mathematical, Physical and Engineering Sciences*, vol. 368, no. 1911, pp. 319–341, 2010.

[25] A. S. Shiriaev, L. B. Freidovich, and S. V. Gusev, "Transverse linearization for controlled mechanical systems with several passive degrees of freedom," *IEEE Trans. Autom. Control*, vol. 55, no. 4, pp. 893–906, 2010.

[26] E. A. Coddington and N. Levinson, *Theory of ordinary differential equations*. Tata McGraw-Hill Education, 1955.

[27] Y. A. Kuznetsov, *Elements of applied bifurcation theory*. Springer Science & Business Media, 2004, vol. 112.

[28] Y. Liu, J. Li, and W. Huang, *Planar dynamical systems: selected classical problems*. De Gruyter, 2014.

[29] M. Guay and T. Zhang, "Adaptive extremum seeking control of nonlinear dynamic systems with parametric uncertainties," *Automatica*, vol. 39, no. 7, pp. 1283–1293, 2003.